NOAA Atlas NESDIS 86

WORLD OCEAN ATLAS 2018
Volume 6: Conductivity

Silver Spring, MD
October 2019

U.S. DEPARTMENT OF COMMERCE
National Oceanic and Atmospheric Administration
National Environmental Satellite, Data, and Information Service

NOAA National Centers for Environmental Information

Additional copies of this publication, as well as information about NCEI data holdings and services, are available upon request directly from NCEI.

NOAA/NESDIS
National Centers for Environmental Information
SSMC3, 4th floor
1315 East-West Highway
Silver Spring, MD 20910-3282

Telephone: (301) 713-3277
E-mail: NCEI.Info@noaa.gov
WEB: http://www.nodc.noaa.gov/

For updates on the data, documentation, and additional information about the WOA18 please refer to:

http://www.nodc.noaa.gov/OC5/indprod.html

This document should be cited as:

Reagan, J.R., M.M. Zweng, D. Seidov, T.P. Boyer, R.A. Locarnini, A.V. Mishonov, O.K. Baranova, H.E. Garcia, K.W. Weathers, C.R. Paver, I.V. Smolyar, and R.H. Tyler (2019). World Ocean Atlas 2018, Volume 6: Conductivity. A. Mishonov Technical Editor, *NOAA Atlas NESDIS 86,* 38 pp.

This document is available on line at http://www.nodc.noaa.gov/OC5/indprod.html

NOAA Atlas NESDIS 86

WORLD OCEAN ATLAS 2018
Volume 6: Conductivity

James R. Reagan, Melissa M. Zweng, Dan Seidov, Timothy P. Boyer, Ricardo A. Locarnini, Alexey V. Mishonov, Olga K. Baranova, Hernan E. Garcia, Katharine W. Weathers, Christopher R. Paver, Igor V. Smolyar, Robert H. Tyler

Technical Editor: Alexey Mishonov

Ocean Climate Laboratory
National Centers for Environmental Information

Silver Spring, Maryland
October, 2019

U.S. DEPARTMENT OF COMMERCE
Wilbur L. Ross, Secretary

National Oceanic and Atmospheric Administration
Neil A. Jacobs, Ph.D.
Assistant Secretary of Commerce for Environmental Observation and Prediction
Acting Under Secretary of Commerce for Oceans and Atmosphere

National Environmental Satellite, Data and Information Service
Stephen Volz, Ph. D.
Assistant Administrator

To Sydney (Syd) Levitus

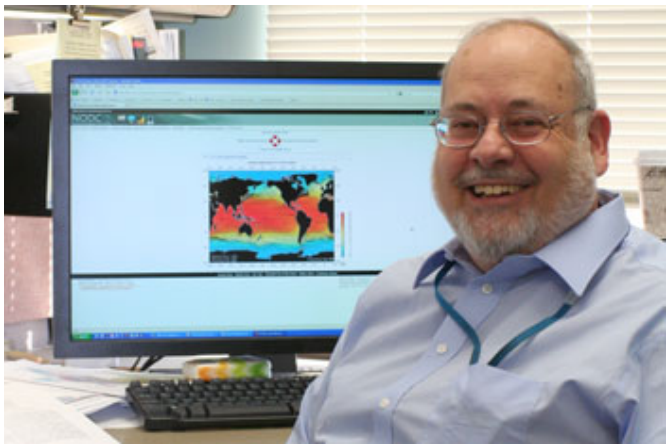

Syd exemplifies the craft of careful, systematic inquiry of the large-scale distributions and low-frequency variability from seasonal-to-decadal time scales of ocean properties. He was one of the first to recognize the importance and benefits of creating objectively analyzed climatological fields of measured ocean variables including temperature, salinity, oxygen, nutrients, and derived fields such as mixed layer depth. Upon publishing *Climatological Atlas of the World Ocean* in 1982, he distributed this work without restriction, an act not common at the time. This seminal atlas moved the oceanographic diagnostic research from using hand-drawn maps to using objectively analyzed fields of ocean variables.

With his NODC Ocean Climate Laboratory (OCL) colleagues, and unprecedented cooperation from the U.S. and international ocean scientific and data management communities, he created the *World Ocean Database (WOD)*; the world's largest collection of ocean profile data that are available internationally without restriction. The *World Ocean Atlas (WOA)* series represents the gridded objective analyses of the WOD and these fields have also been made available without restriction.

The WOD and WOA series are used so frequently that they have become known generically as the "Levitus Climatology". These databases and products enable systematic studies of ocean variability in its climatological context that were not previously possible. His foresight in creating WOD and WOA has been demonstrated by their widespread use over the years. Syd has made major contributions to the scientific and ocean data management communities. He has also increased public understanding of the role of the oceans in climate. He retired in 2013 after 39 years of distinguished civil service. He distilled the notion of the synergy between rigorous data management and science; there are no shortcuts.

All of us at the Ocean Climate Laboratory would like to dedicate this atlas to Syd, his legacy, vision, and mentorship.

The OCL team members

Table of Contents

TABLE OF CONTENTS ..... **I**
LIST OF FIGURES ..... **I**
LIST OF TABLES ..... **I**
PREFACE ..... **III**
ACKNOWLEDGMENTS ..... **IV**
ABSTRACT **1**
1. INTRODUCTION **1**
2. DATA AND DATA DISTRIBUTION **3**
2.1. DATA SOURCES 3
2.2. DATA QUALITY CONTROL 3
2.2.1. Duplicate elimination *4*
2.2.2. Range and gradient checks *4*
2.2.3. Statistical checks *5*
2.2.4. Static stability check *5*
2.2.5. Subjective flagging of data *6*
2.2.6. Representativeness of the data *6*
2.2.7. XCTD drop-rate error correction *7*
2.3. CONDUCTIVITY DERIVATION 7
3. DATA PROCESSING PROCEDURES **8**
3.1. VERTICAL INTERPOLATION TO STANDARD LEVELS 8
3.2. METHODS OF ANALYSIS 9
3.2.1. Overview *9*
3.2.2. Derivation of Barnes (1964) weight function *10*
3.2.3. Derivation of Barnes (1964) response function *11*
3.2.4. Choice of response function *12*
3.2.5. First-guess field determination *13*
3.3. CHOICE OF OBJECTIVE ANALYSIS PROCEDURES 14
3.4. CHOICE OF SPATIAL GRID 14
3.4.1 Increased Spatial Resolution *15*
4. RESULTS **16**
4.1. COMPUTATION OF ANNUAL AND SEASONAL FIELDS 17
4.2. AVAILABLE STATISTICAL FIELDS 17
4.3 OBTAINING WOA18 FIELDS ONLINE 17
5. SUMMARY **17**
6. FUTURE WORK **18**
7. REFERENCES **18**

List of Figures

Figure 1. The annual conductivity of the Gulf Stream at 0m depth for the 2005 - 2017 decade as represented by one-degree resolution and quarter-degree resolution. ..... **Error! Bookmark not defined.**
Figure 2. Response function of the WOA18, WOA13, WOA09, WOA05, WOA01, WOA98, WOA94, and Levitus (1982) objective analysis schemes. 29
Figure 3. Scheme used in computing "all-data" annual, seasonal, and monthly objectively analyzed means for conductivity. 30

List of Tables

Table 1. Radii of influence used in the objective analysis for the one-degree and quarter-degree climatologies 15
Table 2. Descriptions of climatologies for conductivity. The standard depth levels are shown in Table 4. 23

Table 3. Descriptions of datasets in WOD18.....23
Table 4. Acceptable distances (m) for defining interior (A) and exterior (B) values used in the Reiniger-Ross scheme for interpolating observed level data to standard levels. 24
Table 5. Response function of the objective analysis scheme as a function of wavelength for WOA18 and earlier analyses. Response function is normalized to 1.0. 26
Table 6. Basins defined for objective analysis and the shallowest standard depth level for which each basin is defined.....27
Table 7. Statistical fields calculated as part of WOA18 Conductivity.....28

Preface

The World Ocean Atlas 2018 (WOA18) is the latest in a line of oceanographic analyses of subsurface ocean variables at standard depths extending back to the groundbreaking *Climatological Atlas of the World Ocean* (Levitus, 1982). The WOA has been published semi-regularly since 1994, with versions in 1998, 2001, 2005, 2009, 2013, and now 2018. Previous iterations of the WOA have proven to be of great utility to the oceanographic, climate research, geophysical, and operational environmental forecasting communities. The oceanographic variable analyses are used as boundary and/or initial conditions in numerical ocean circulation models and atmosphere-ocean models, for verification of numerical simulations of the ocean, as a form of "sea truth" for satellite measurements such as altimetric observations of sea surface height, for computation of nutrient fluxes by Ekman transport, and for planning oceanographic expeditions among others.

WOA18 includes analyses on a one-degree grid for all variables and on a quarter-degree grid for temperature and salinity. Since WOA13, the ocean variable analyses are produced on 102 depth levels from the surface to 5,500 m (previously 33 levels within the same depth limits). Ocean data and analyses of data at higher vertical resolution than previously available are needed to document the variability of the ocean, including improving diagnostics, understanding, and modeling of the physics of the ocean.

In the acknowledgment section of this publication, we have expressed our view that creation of global ocean profile and plankton databases and analyses are only possible through the cooperation of scientists, data managers, and scientific administrators throughout the international scientific community.

A pre-release version of WOA18 was made available in September, 2018. The final version of WOA18 was released in July, 2019. In the interim, community feedback and our own work has led to changes in the temperature atlas in particular. Animal mounted pinniped temperature profiles have been added as a data source improving coverage in some high latitude areas. A different Expendable Bathythermograph (XBT) correction (Cheng et al., 2014) has been employed. These changes are detailed below. Also, the XBTs were doubly corrected in the pre-release version. The Levitus correction was applied after another correction had been applied (Cheng et al., 2014). This error led to an ocean which was less than 0.1°C cooler in the pre-release WOA18 as compared to the final WOA18 for the most affected decades (1975-84, 1985-94, 1995-2004) in the upper 400m with smaller differences below. The 1981-2010 climate normal for temperature is slightly cooler (< 0.05°C) in the final WOA18 than in the pre-release WOA18 due to inadvertent double-weighting of the 2001-2010 decade in the pre-release version.

Ocean Climate Laboratory Team
National Centers for Environmental Information
Silver Spring, MD
October 2019

Acknowledgments

This work was made possible by a grant from the NOAA Climate and Global Change Program, which enabled the establishment of a research group at the National Oceanographic Data Center (now the National Centers for Environmental Information – NCEI). The purpose of this group is to prepare research quality oceanographic databases, as well as to compute objective analyses of, and diagnostic studies based on, these databases. Support is now from base funds and from the NOAA Climate Program Office.

The data on which this atlas is based are in *World Ocean Database 2018* and are distributed on-line by NCEI. Many data were acquired as a result of the IOC/IODE *Global Oceanographic Data Archaeology and Rescue* (GODAR) project, and the IOC/IODE *World Ocean Database* project (WOD). At NCEI and the World Data System for Oceanography, data archaeology and rescue projects were supported with funding from the NOAA Environmental Science Data and Information Management (ESDIM) Program and the NOAA Climate and Global Change Program which has included support from NASA and DOE. Support for some of the regional IOC/GODAR meetings was provided by the Marine Science and Technology (MAST) program of the European Union. The European Community has also provided support for the Mediterranean Data Archeology and Rescue (MEDAR/MEDATLAS) Project, which has resulted in the inclusion of substantial amounts of ocean profile data from the Mediterranean Sea. Additional Black Sea data have been acquired as a result of a NATO sponsored project.

We acknowledge the scientists, technicians, and programmers who have collected and processed data, those individuals who have submitted data to national and regional data centers as well as the managers and staff at the various data centers. We are working on a more substantive and formalized way to acknowledge all those who have collected and contributed to oceanographic measurements, which were used to calculate the fields in the WOA. Until we have such a system in place, we direct the reader's attention to lists of primary investigators, institutions, and projects, which contributed data (codes can be used to locate data in the World Ocean Database). We also thank our colleagues at the NCEI. Their efforts have made this and similar works possible.

We dedicate this work to Carla Coleman who always contributed with a smile and was taken from us too soon.

WORLD OCEAN ATLAS 2018
Volume 6: Conductivity

ABSTRACT

This atlas consists of a description of data analysis procedures and horizontal maps of climatological distribution fields of electrical conductivity at selected standard-depth levels of the World Ocean on one-degree and quarter-degree latitude-longitude grids. The aim of the maps is to illustrate large-scale characteristics of the distribution of ocean conductivity. The fields used to generate these climatological maps were computed by objective analysis of historical conductivity data that were derived from scientifically quality-controlled temperature and salinity data in the *World Ocean Database 2018*. Maps are presented for climatological composite periods (annual, seasonal, monthly, seasonal and monthly difference fields from the annual mean field, and the number of observations) at 102 standard depths.

1. INTRODUCTION

This atlas is part of the *World Ocean Atlas 2018* (WOA18) series. The WOA18 series includes analysis for temperature (Locarnini *et al.*, 2019); salinity (Zweng *et al.,* 2019); dissolved oxygen (Garcia *et al.*, 2019a); and dissolved inorganic nutrients (Garcia *et al.*, 2019b). This atlas presents annual, seasonal, and monthly climatologies and related statistical fields for conductivity. Climatologies in this atlas are defined as mean oceanographic fields at selected standard depth levels based on the objective analysis of historical oceanographic profiles and select surface-only data. A profile is defined as a set of measurements for a single variable (temperature, salinity, *etc*.) at discrete depths taken as an instrument drops or rises vertically in the water column.

Since the 1970's seawater electrical conductivity is typically measured to determine salinity, but the conductivity is often not reported. Therefore, to create conductivity profiles, concurrent temperature, salinity, and pressure measurements were used to derive the conductivity of seawater. These profiles of conductivity are then used in creating the conductivity climatologies.

The annual "all-data" conductivity climatology was calculated using observations from all months for the 1978-2017 time period. Seasonal "all-data" climatologies were calculated using only data from the defined season within the 1978-2017 time period. The seasons are defined as follows: Winter is defined as January, February, and March; spring as April, May, and June; summer as July, August, and September; and fall as October, November, and December. Monthly "all-data" climatologies were calculated using data only from the given month within the 1978-2017 time period. The reason why the 1978-2017 time period is used for the "all-data" climatologies is explained in 2.3.

The conductivity data used to calculate the climatologies are derived from concurrently measured temperature, salinity, and pressure data available from the National Centers for Environmental Information (NCEI) and World Data Center (WDC) for Oceanography, Silver Spring, Maryland. Large volumes of data have been acquired as a result of the fulfillment of several data

management projects including:

a) the Intergovernmental Oceanographic Commission (IOC) Global Oceanographic Data Archaeology and Rescue (GODAR) project (Levitus *et al.*, 2005);
b) the IOC World Ocean Database project (WOD);
c) the IOC Global Temperature Salinity Profile project (GTSPP) (IOC, 1998).

The conductivity data used in the WOA18 have been analyzed in a consistent, objective manner on one-degree and quarter-degree latitude-longitude grids at standard depth levels from the surface to a maximum depth of 5500m. The procedures for "all-data" climatologies are identical to those used in the *World Ocean Atlas 2013* (WOA13) series (Johnson *et al*., 2013, Locarnini *et al*. 2013, Zweng *et al*., 2013), *World Ocean Atlas 2009* (WOA09) series (Locarnini *et al*., 2010; Antonov *et al*., 2010; Garcia *et al*. 2010 a, b), *World Ocean Atlas 2005* (WOA05) series (Locarnini *et al*., 2006; Antonov *et al*., 2006; Garcia *et al*. 2006 a, b), the *World Ocean Atlas 2001* (WOA01) series (Stephens *et al.*, 2002; Boyer *et al*., 2002; Locarnini *et al.*, 2002; Conkright *et al*., 2002) and *World Ocean Atlas 1998* (WOA98) series (Antonov *et al*., 1998 a, b, c; Boyer *et al*., 1998 a, b, c; Conkright *et al*., 1998, a, b, c; O'Brien *et al*., 1998, a, b, c) with the slight difference for conductivity in that "all-data" refers to the 1978-2017 time period and not the full historical period available in the WOD. Slightly different procedures were followed in earlier analyses (Levitus, 1982; *World Ocean Atlas 1994* series [WOA94, Levitus *et al*., 1994; Levitus and Boyer 1994a, b; Conkright *et al*., 1994]). WOA13 differed from WOA09 by increasing the number of standard levels used from 33 to 102, increasing the resolution with depth; WOA18 continues to use the same 102 depth levels as WOA13.

Objective analyses shown in this atlas are limited by the nature of the temperature and salinity databases (data are non-uniform in both space and time), characteristics of the objective analysis techniques, and the grid used. Additionally, because conductivity is a derived quantity based on temperature, salinity, and pressure, profiles of conductivity can only be calculated for profiles that have concurrent temperature and salinity measurements. Thus, the primary limitation of the analysis is data coverage in space and time. Since the publication of WOA13, substantial amounts of additional historical concurrently measured temperature and salinity data have become available. However, even with these additional data, we are still hampered in a number of ways by a lack of data. In some areas, quality control is made difficult by the limited number of data collected in these areas. Data may exist in an area for only one season, thus precluding any representative annual analysis. In some areas there may be a reasonable spatial distribution of data points on which to base an analysis, but there may be only a few (perhaps only one) data values in each one-degree latitude-longitude square.

While electrical conductivity is not usually a parameter of direct interest in the primary studies of the ocean's fluid- and thermo-dynamics, it is a fundamental parameter in the ocean's electrodynamics. The conductivity is needed both in forward modeling of ocean electrodynamic processes (e.g. charge separation, induction, and motional induction) and in the interpretation of ocean flow, temperature, and salinity using in situ and remote electric and magnetic field observations. This can include traditional interpretation of in situ electric fields to infer flow velocity, as well as potential new opportunities such as the inference of ocean heat content using satellite magnetometers (Tyler and Sabaka, 2016; Trossman and Tyler, 2019; Irrgang *et al.,* 2019).

Conductivity was first added to the WOA13 climatology (Tyler, et. al., 2017) and is extended here in WOA18.

This atlas is divided into sections. We begin by describing the data sources and data distribution (Section 2). Then we describe the general data processing procedures (Section 3), the results (Section 4), summary (Section 5), future work (Section 6), and references (Section 7). Maps for each individual depth level for each time period are available online.

2. DATA AND DATA DISTRIBUTION

Data sources and quality control procedures are briefly described below. For further information on the data sources used in WOA18 refer to the *World Ocean Database 2018* (WOD18, Boyer *et al.*, 2019). The quality control procedures used in preparation of these analyses are described by Garcia *et al*. (2019).

2.1. Data sources

Historical oceanographic temperature and salinity profile data from bottle samples, ship-deployed Conductivity-Temperature-Depth (CTD) packages, profiling floats, moored and drifting buoys, gliders, and undulating oceanographic recorder (UOR) profiles used in this project were obtained from the NCEI/WDS archives and include all data gathered as a result of the GODAR and WOD projects.

To understand the procedures for taking individual oceanographic observations and constructing climatological fields, it is necessary to define the terms "standard level data" and "observed level data". We refer to the actual measured value of an oceanographic variable *in situ* as an "observation", and to the depth at which such a measurement was made as the "observed level depth." We refer to such data as "observed level data." Before the development of oceanographic instrumentation that measures at high frequencies along the vertical profile, oceanographers often attempted to make measurements at selected "standard levels" in the water column. Sverdrup et al. (1942) presented the suggestions of the International Association for the Physical Sciences of the Oceans (IAPSO) as to which depths oceanographic measurements should be made or interpolated to for analysis. Historically the World Ocean Atlas used a modified version of the IAPSO standard depths. However, with the increased global coverage of high depth resolution instrumentation, such as profiling floats, WOA has extended the standard depth levels from 33 to 102. The current standard depth levels include the original depth levels presented up to WOA09, but have tripled the resolution in the upper 100 meters, more than doubled the depth resolution of the upper 1000 meters, and nearly quadrupled the depth resolution below 1000 meters. For many purposes, including preparation of the present climatologies, observed level data are interpolated to standard depth levels if observations did not occur at the desired standard depths (see section 3.1 for details). The levels at which the climatologies were calculated are given in Table 2. Table 3 describes the datasets used to calculate the climatologies. Table 4 shows the depths of each standard depth level.

2.2. Data quality control

Quality control of the temperature and salinity data is a major task, the difficulty of which is directly related to lack of data and metadata (for some areas) upon which to base statistical checks. Consequently, certain empirical criteria were applied - see sections 2.2.1 through 2.2.4, and as part of the last processing step, subjective judgment was used - see sections 2.2.5 and 2.2.6. Individual

salinity and temperature data, and in some cases entire profiles or all profiles for individual cruises, have been flagged and not used further because these data produced features that were judged to be non-representative or questionable. As part of our work, we have made available WOD18 that contains both observed levels profile data and standard depth level profile data with various quality control flags applied. The flags mark either individual measurements or entire profiles that were not used in the next step of the procedure-- either interpolation to standard depth levels for observed level data or calculation of statistical means in the case of standard depth level data.

Constantly improving knowledge of the world ocean variability now includes a greater appreciation and understanding of the ubiquity of mesoscale features such as eddies, rings, and lenses in some parts of the world ocean, as well as interannual and multi-decadal variability of water mass properties associated with modal variability of the atmosphere such as the North Atlantic Oscillation (NAO) and El Niño Southern Ocean Oscillation (ENSO). Some of these features, especially in the region with dense data coverage like, for example the Northwest Atlantic Ocean, can find their way into high-resolution analyses and lead to a cumulative effect of mesoscale dynamics seen in decadal climatologies (Seidov et al, 2018); see below about weakened restriction on outlier flagging in coastal areas. However, in most regions with lesser data coverage, these features seen as outliers may not be consistent with the background WOA fields, but still represent legitimate data values. Therefore, we have simply flagged these data, if seen as obvious outliers, but have not removed them from the WOD18. Thus, individual investigators can make their own decision regarding the representativeness of the data. Investigators studying the distribution of features such as eddies will be interested in those data that we may regard as unrepresentative for the preparation of the analyses shown in this atlas. Likewise, investigators who want to use the conductivity data to constrain boundary and/or initial conditions at non-eddy-resolving resolutions may opt to exclude the flagged data.

2.2.1. Duplicate elimination

Because temperature and salinity data are received from many sources, sometimes the same data set is received at NCEI/WDC more than once but with slightly different time and/or position and/or data values, and hence are not easily identified as duplicate stations. Therefore, to eliminate the repetitive data values our databases were checked for the presence of exact and "near" exact replicates using eight different criteria. The first checks involve identifying stations with exact position/date/time and data values; the next checks involve offsets in position/date/time. Profiles identified as duplicates in the checks with a large offset were individually verified to ensure they were indeed duplicate profiles.

All but one profile from each set of duplicate profiles were eliminated at the first step of our processing.

2.2.2. Range and gradient checks

Range checking (that is, checking whether a salinity and/or temperature value is within preset minimum and maximum values as a function of depth and ocean region) was performed on all temperature and salinity values as a first quality control check to flag and withhold from further use the relatively few values that were grossly outside expected oceanic ranges. Range checks were prepared for individual regions of the world ocean. Boyer *et al.* (2019) and Boyer and Levitus (1994) detail the quality control procedures. Range tables showing the temperature and

salinity ranges selected for each basin and depth can be found in Boyer *et al*. (2019).

A check as to whether excessive vertical gradients occur in the data has been performed for each variable in WOD18 both in terms of positive and negative gradients. See Boyer *et al.* (2019) for limits for excessive gradients for temperature and salinity.

2.2.3. Statistical checks

Statistical checks were performed on the data according to the following procedure. All data for temperature and salinity (irrespective of year), at each standard depth level, were averaged within five-degree latitude-longitude squares to produce a record of the number of observations, mean, and standard deviation in each square. Statistics were computed for the annual, seasonal, and monthly compositing periods. Below 50 m depth, if data were more than three standard deviations from the mean, the data were flagged and withheld from further use in objective analyses. Above 50 m depth, a five-standard-deviation criterion was used in five-degree squares that contained any land area. In selected five-degree squares that are close to land areas, a four-standard-deviation check was used. In all other squares a three-standard-deviation criterion was used for the 0-50 m depth layer. For standard depth levels situated directly above the bottom, a four-standard-deviation criterion was used.

The reason for the weaker standard deviation criterion in coastal and near-coastal regions is the exceptionally large variability in the coastal five-degree square statistics for some variables. Frequency distributions of some variables in some coastal regions are observed to be skewed or bimodal. Thus, to avoid eliminating possibly good data in highly variable environments, the standard deviation criteria were broadened.

The total number of measurements in each profile and the total number of temperature and salinity observations exceeding the criterion is recorded. If more than four standard level values in a profile were found to exceed the standard deviation criterion, then the entire profile was flagged. This check was imposed after tests indicated that surface data from particular casts (which upon inspection appeared to be erroneous) were being flagged but deeper data were not. Other situations were found where erroneous data from the deeper portion of a cast were flagged, while near-surface data from the same cast were not flagged because of larger natural variability in surface layers. One reason for this was the decrease of the number of observations with depth and the resulting change in sample statistics. The standard-deviation check was applied twice to the data set for each compositing period.

In summary, first the five-degree square statistics were computed, and the data flagging procedure described above was used to provide a preliminary data set. Next, new five-degree-square statistics were computed from this preliminary data set and used with the same statistical check to produce a new, "clean" data set. The reason for applying the statistical check twice was to flag (and withhold from further use), in the first round, any grossly erroneous or non-representative data from the data set that would artificially increase the variances. The second check is then more effective in identifying values with smaller differences that are still non-representative.

2.2.4. Static stability check

Each cast containing both temperature and salinity was checked for static stability as defined by Hesselberg and Sverdrup (1914). Neumann and Pierson (1966, p. 139) reviewed this definition. The computation is a "local" one in the sense that adiabatic displacements between adjacent temperature-

salinity measurements in the vertical are considered rather than displacements to the sea surface. Lynn and Reid (1968) discussed the reasons for use of the local stability computation. The procedure for computation follows that used by Lynn and Reid (1968) and is given by:

$$E = \lim_{\partial z \to 0} \frac{1}{\rho_0} \frac{\delta \rho}{\partial z} \qquad (1)$$

in which: $\rho_o = 1.02*10^3$ kg·m^{-3}. As noted by Lynn and Reid, the term "is the individual density gradient defined by vertical displacement of a water parcel (as opposed to the geometric density gradient). For discrete samples the density difference ($\delta\rho$) between two samples is taken after one is adiabatically displaced to the depth of the other". For the results at any standard level (k), the computation was performed by displacing parcels at the next deeper standard level ($k+l$) to level k.

The actual procedure for using stability checks to flag sets of data points was as follows. To a depth of 30 m, stability (E) inversions in excess of $3 \cdot 10^{-5}$g·cm^{-3} were flagged, and below this depth down to the 400m level, inversions in excess of $2 \cdot 10^{-5}$g·cm^{-3} were flagged. Below 400m any inversion was flagged. To eliminate an inversion both temperature and salinity were flagged and excluded from further use at both standard levels involved in the computation. In the actual processing a count was kept of the number of inversions in each cast. If a cast had two or more unacceptable inversions, as defined above, then the entire cast was eliminated from further use.

2.2.5. Subjective flagging of data

Analysis for WOA18 was done on two grids: a one-degree grid and a quarter-degree grid. For the one-degree analysis, the derived conductivity data were averaged by one-degree squares for input to the objective analysis program. After initial objective analyses were computed, the input set of one-degree means still contained questionable data contributing to unrealistic distributions, yielding intense bull's-eyes or spatial gradients. Examination of these features indicated that some of them were due to profiles from particular oceanographic cruises. In such cases, data from an entire cruise were flagged and withheld from further use by setting a flag on each profile from the cruise. In other cases, individual profiles or measurements were found to cause these features and were flagged. For the quarter-degree analysis, the same procedure was repeated on a finer quarter-degree grid.

2.2.6. Representativeness of the data

Another quality control issue is data representativeness. The general paucity of data forces the compositing of all historical data, or in the case of conductivity years 1978-2017, to produce "climatological" fields. In a given grid square, there may be data from a month or season of one particular year, while in the same or a nearby square there may be data from an entirely different year. If there is large interannual variability in a region where scattered sampling in time has occurred then one can expect the analysis to reflect this. Because the observations are scattered randomly with respect to time, except for a few limited areas, the results cannot, in a strict sense, be considered a true long-term climatological average.

For the present atlas we attempted to reduce the effects of irregular space-time sampling by the averaging of three “climatologies” computed for the following time periods: 1981-1990, 1991-2000, and 2001-2010. These three periods averaged together yields a 1981-2010 climatology, commonly referred to as the latest “climate normal” period which allows for comparisons with other works. The first-guess field for each of these

climatologies is the "all-data" (1978-2017) objectively analyzed conductivity field. Additionally, a 2005-2017 decadal conductivity climatology is also provided as this decade provides a sufficient number of concurrent temperature, salinity, and pressure measurements allowing conductivity to be calculated and a climatology to be developed.

We present smoothed analyses of historical means, based (in certain areas) on relatively few observations. We believe, however, that useful information about the oceans can be gained through our procedures and that the large-scale features are representative of the real ocean.

The data diminish in number with increasing depth. In the upper ocean, the all-data annual mean distributions are sufficient for defining large-scale features, but the database is inadequate in some regions for the seasonal periods. In some areas of the deep ocean, the distribution of observations may be adequate for some diagnostic computations but inadequate for other purposes. If an isolated deep basin or some region of the deep ocean has only one observation, then no horizontal gradient computations are meaningful. However, useful information is provided by the observation in the computation of other quantities (*e.g.* a volumetric mean over a major ocean basin).

2.2.7. XCTD drop-rate error correction

Johnson (1995) has shown the necessity of depth correction for Sippican XCTDs, while Mizuno and Watanabe (1998) and Koso *et al*. (2005) give depth corrections for TSK XCTDs. Kizu *et al*. (2008) find that the TSK manufacturer's drop rate as corrected according to these works is generally satisfactory. **We have made no correction to the depths of the observed level XCTD profiles**. Thus, investigators, if they desire, can make whatever correction they need to the observed level data we are providing since we have not corrected these profiles for this error. However, in order to merge Sippican and TSK XCTD data with other types of temperature and salinity measurements, and in order to produce climatologies and other analyses, by necessity we have corrected the drop-rate error in these XCTD profiles, as part of the process of interpolating the data to standard depth levels (the drop-rate correction was applied to the observed level data before interpolation to standard levels). **All Sippican and TSK XCTD profiles that we have used in generating products at standard levels, or made available as part of our standard level profile data sets, have been corrected for the drop-rate error**. **If users wish to use another procedure, but still use the XCTD data set we have compiled, they can do so by applying their correction procedure to our observed level XCTD profile data set, which has not been corrected for the drop-rate error**.

2.3. Conductivity Derivation

As noted previously, for this atlas, conductivity is a derived variable based on concurrent measurements of temperature, salinity, and pressure. Once all temperature and salinity quality control checks are completed (e.g., duplication checks, statistical checks, stability checks, etc.; see section 2.2), conductivity is computed for each profile at each observed depth level for which there are concurrent measurements of temperature and salinity that passed all levels of quality control. The derived conductivity is calculated using the gsw_C_from_SP FORTRAN subroutine in the Gibbs Seawater Toolbox of the Thermodynamic Equation of Seawater (TEOS-10) (McDougall and Barker, 2011; IOC *et al.,* 2010). The inputs for this subroutine include salinity (reported on the Practical Salinity Scale of 1978), temperature (reported on the International

Temperature Scale of 1990), and pressure (dbar). The basic conductivity equation is as follows:

$$C(S_p, t_{68}, p) = C(35{,}15°\text{C}, 0\text{ dbar}) * R \quad (2)$$

where $C(S_p, t_{68}, p)$ is the conductivity to be calculated in Siemens/meter (S/m), $C(35{,}15°\text{C}, 0\text{ dbar})$ is a constant (4.29140 S/m), and R is the conductivity ratio (unitless). For information on the solution to R please see McDougall and Barker (2011), IOC *et al.* (2010) and Tyler *et al.* (2017). Equation (2) is only applicable for salinity values ranging from 2 to 42. However, the Gibbs Seawater Toolbox accounts for salinities less than 2 by using the methods developed by Hill *et al.* (1986). Finally, the conversion between temperatures reported on the International Practical Temperature Scale (IPTS) of 1968 and ITS-90 is: $t_{68} = 1.00024 \times t_{90}$.

If pressure is not known, and only the depth (in meters) is, we estimated pressure using the GSW subroutine gsw_p_from_z which requires latitude and depth as inputs. With the requirement that the salinity be reported on the PSS-78 scale, we derived conductivity profiles for only the years 1978-2017, the time period for which we are confident that salinity is reported on the correct scale (PSS-78).

Once the conductivity is calculated for each profile, it goes through additional rounds of quality control. These include both statistical checks (see 2.2.3) and subjective checks (see 2.2.5). As discussed in 2.2.6, conductivity climatologies for 1981-2010 (latest "climate normal" time period) and 2005-2017 are only calculated due to the spatial and temporal availability of concurrent measurements of temperature and salinity.

3. DATA PROCESSING PROCEDURES

3.1. Vertical interpolation to standard levels

Vertical interpolation of observed depth level data to standard depth levels followed procedures in JPOTS Editorial Panel (1991). These procedures are in part based on the work of Reiniger and Ross (1968). Four observed depth level values surrounding the standard depth level value were used, two values from above the standard level and two values from below the standard level. The pair of values furthest from the standard level is termed "exterior" points and the pair of values closest to the standard level is termed "interior" points. Paired parabolas were generated via Lagrangian interpolation. A reference curve was fitted to the four data points and used to define unacceptable interpolations caused by "overshooting" in the interpolation. When there were too few data points above or below the standard level to apply the Reiniger and Ross technique, we used a three-point Lagrangian interpolation. If three points were not available (either two above and one below or vice-versa), we used linear interpolation. In the event that an observation occurred exactly at the depth of a standard level, then a direct substitution was made. Table 4 provides the range of acceptable distances for which observed level data could be used for interpolation to a standard level.

WOD13 increased the number of standard levels from 33 to 102, allowing for analysis with greater vertical resolution. WOA18 also uses 102 standard depth levels. The method for interpolating data to standard levels remains the same as previous analyses.

Conductivity is derived from the observed level temperature and salinity measurements of a profile and therefore it is the calculated conductivity at observed levels that is vertically interpolated to standard levels. We do not use the standard level temperature and salinity data to compute the standard level conductivity data.

3.2. Methods of analysis

3.2.1. Overview

An objective analysis scheme of the type described by Barnes (1964) was used to produce the fields shown in this atlas. This scheme had its origins in the work of Cressman (1959). In *World Ocean Atlas 1994* (WOA94), the Barnes (1973) scheme was used. This required only one "correction" to the first-guess field at each grid point in comparison to the successive correction method of Cressman (1959) and Barnes (1964). This was to minimize computing time used in the processing. Barnes (1994) recommends a return to a multi-pass analysis when computing time is not an issue. Based on our own experience we agree with this assessment. The single pass analysis, used in WOA94, caused an artificial front in the Southeastern Pacific Ocean in a data sparse area (Anne Marie Treguier, personal communication). The analysis scheme used in generating WOA98, WOA01, WOA05, WOA09, WOA13, and WOA18 analyses uses a three-pass "correction" which does not result in the creation of this artificial front.

The analysis was performed on both the one-degree and quarter-degree grids. Inputs to the analysis scheme were one grid square means of data values at standard levels (for time period and variable being analyzed), and a first-guess value for each square. For instance, grid-square means for our "all-data" annual analysis were computed using all available data regardless of date of observation. For "all-data" July, we used all historical July data regardless of year of observation. "All-data" for conductivity only refers to the time period of 1978 through 2017. For "decadal" July, we used July data only collected within a specified decade.

Analysis was the same for all standard depth levels. Each one- or quarter-degree latitude-longitude square value was defined as being representative of its square. The dimension of the one-degree grid was 360x180, while the quarter-degree grid was 1440x720. Gridpoints are located at the "centers" of their boxes. An influence radius was then specified. At those gridpoints where there was an observed mean value, the difference between the mean and the first-guess field was computed. Next, a correction to the first-guess value at all gridpoints was computed as a distance-weighted mean of all gridpoint difference values that lie within the area around the gridpoint defined by the influence radius. Mathematically, the correction factor derived by Barnes (1964) is given by the expression:

$$C_{i,j} = \frac{\sum_{s=1}^{n} W_s Q_s}{\sum_{s=1}^{n} W_s} \qquad (3)$$

in which:

(i,j) - coordinates of a gridpoint in the east-west and north-south directions respectively;

$C_{i,j}$ - the correction factor at gridpoint coordinates (i,j);

n - the number of observations that fall within the area around the point i,j defined by the influence radius;

Q_s - the difference between the observed mean and the first-guess at the Sth point in the influence area;

$W_s = e^{-\frac{Er^2}{R^2}}$ (for $r \leq R$; $W_s = 0$ for $r > R$);

r - distance of the observation from the gridpoint;

R - influence radius;

$E = 4$.

The derivation of the weight function, W_s, will be presented in the following section. At each gridpoint we computed an analyzed

value $G_{i,j}$ as the sum of the first-guess, $F_{i,j}$, and the correction $C_{i,j}$. The expression for this is

$$G_{i,j} = F_{i,j} + C_{i,j} \tag{4}$$

If there were no data points within the area defined by the influence radius, then the correction was zero, the first-guess field was left unchanged, and the analyzed value was simply the first-guess value. This correction procedure was applied at all gridpoints to produce an analyzed field. The resulting field was first smoothed with a median filter (Tukey, 1974; Rabiner *et al.,* 1975) and then smoothed with a five-point smoother of the type described by Shuman (1957) (hereafter referred as five-point Shuman smoother). The choice of first-guess fields is important and we discuss our procedures in section 3.2.5.

The analysis scheme is set up so that the influence radius, and the number of five-point smoothing passes can be varied with each iteration. The strategy used is to begin the analysis with a large influence radius and decrease the radius with each iteration. This technique allows us to analyze progressively smaller size phenomena.

The analysis scheme is based on the work of several researchers analyzing meteorological data. Bergthorsson and Doos (1955) computed corrections to a first-guess field using various techniques: one assumed that the difference between a first-guess value and an analyzed value at a gridpoint was the same as the difference between an observation and a first-guess value at a nearby observing station. All the observed differences in an area surrounding the gridpoint were then averaged and added to the gridpoint first-guess value to produce an analyzed value. Cressman (1959) applied a distance-related weight function to each observation used in the correction in order to give more weight to observations that occur closest to the gridpoint. In addition, Cressman introduced the method of performing several iterations of the analysis scheme using the analysis produced in each iteration as the first-guess field for the next iteration. He also suggested starting the analysis with a relatively large influence radius and decreasing it with successive iterations so as to analyze smaller scale phenomena with each pass.

Sasaki (1960) introduced a weight function that was specifically related to the density of observations, and Barnes (1964, 1973) extended the work of Sasaki. The weight function of Barnes (1964) has been used here. The objective analysis scheme we used is in common use by the mesoscale meteorological community. Several studies of objective analysis techniques have been made. Achtemeier (1987) examined the "concept of varying influence radii for a successive corrections objective analysis scheme." Seaman (1983) compared the "objective analysis accuracies of statistical interpolation and successive correction schemes." Smith and Leslie (1984) performed an "error determination of a successive correction type objective analysis scheme." Smith *et al*. (1986) made "a comparison of errors in objectively analyzed fields for uniform and non-uniform station distribution."

3.2.2. Derivation of Barnes (1964) weight function

The principle upon which the Barnes (1964) weight function is derived is that "the two-dimensional distribution of an atmospheric variable can be represented by the summation of an infinite number of independent harmonic waves, that is, by a Fourier integral representation". If *f(x,y)* is the variable, then in polar coordinates *(r,θ)*, a smoothed or filtered function *g(x,y)* can be defined:

$$g(x,y) = \frac{1}{2\pi}\int_0^{2\pi}\int_0^{\infty} \eta f(x + r\cos\theta, y + r\sin\theta) d(\frac{r^2}{4K}) d\theta$$

(5)

in which r is the radial distance from a gridpoint whose coordinates are *(x,y)*. The weight function is defined as

$$\eta = e^{-\frac{r^2}{4K}} \qquad (6)$$

which is a Gaussian distribution. The shape of the weight function is determined by the value of K, which relates to the distribution of data. The determination of K follows. The weight function has the property that

$$\frac{1}{2\pi}\int_0^{2\pi}\int_0^{\infty}\eta d\left(\frac{r^2}{4K}\right)d\theta = 1 \qquad (7)$$

This property is desirable because in the continuous case (5) the application of the weight function to the distribution *f(x,y)* will not change the mean of the distribution. However, in the discrete case (3), we only sum the contributions to within the distance R. This introduces an error in the evaluation of the filtered function, because the condition given by (7) does not apply. The error can be pre-determined and set to a reasonably small value in the following manner. If one carries out the integration in (7) with respect to θ, the remaining integral can be rewritten as

$$\int_0^R \eta d\left(\frac{r^2}{4K}\right) + \int_R^{\infty}\eta d\left(\frac{r^2}{4K}\right) = 1 \qquad (8)$$

Defining the second integral as ε yields

$$\int_0^R e^{-\frac{r^2}{4K}} d\left(\frac{r^2}{4K}\right) = 1 - \varepsilon \qquad (9)$$

Integrating (9), we obtain

$$\varepsilon = e^{-\frac{R^2}{4K}} \qquad (9a)$$

Taking the natural logarithm of both sides of (9a) leads to an expression for K,

$$K = R^2 / 4E \qquad (9b)$$

where $E \equiv -\ln \varepsilon$.

Rewriting (6) using (9b) leads to the form of weight function used in the evaluation of (3).

Thus, choice of E and the specification of R determine the shape of the weight function.

Levitus (1982) chose E=4 which corresponds to a value of ε of approximately 0.02. This choice implies with respect to (9) the representation of more than 98 percent of the influence of any data around the gridpoint in the area defined by the influence radius R.

This analysis (WOA18) and previous analyses (WOA94, WOA98, WOA01, WOA05, WOA09, WOA13) used E=4.

Barnes (1964) proposed using this scheme in an iterative fashion similar to Cressman (1959). Levitus (1982) used a four-iteration scheme with a variable influence radius for each pass. As noted earlier, WOA94 used a one-iteration scheme, while WOA98, WOA01, WOA05, WOA09, WOA13 and WOA18 employed a three-iteration scheme with a variable influence radius.

3.2.3. Derivation of Barnes (1964) response function

It is desirable to know the response of a data set to the interpolation procedure applied to it. Following Barnes (1964) and reducing to one-dimensional case we let

$$f(x) = A\sin(\alpha x) \qquad (10)$$

in which $\alpha = 2\pi/\lambda$ with λ being the wavelength of a particular Fourier component, and substitute this function into equation (5) along with the expression for η in equation (6). Then

$$g(x) = D[A\sin(\alpha x)] = Df(x) \qquad (11)$$

in which D is the response function for one application of the analysis and defined as

$$D = e^{-\left(\frac{\alpha R}{4}\right)^2} = e^{-\left(\frac{\pi R}{2\lambda}\right)^2} \qquad (12)$$

The phase of each Fourier component is not changed by the interpolation procedure. The results of an analysis pass are used as the first-guess for the next analysis pass in an iterative fashion. The relationship between the filtered function *g(x)* and the response function after *N* iterations as derived by Barnes (1964) is

$$g_N(x) = f(x) D \sum_{n=1}^{N} (1-D)^{n-1} \qquad (13)$$

Equation (13) differs trivially from that given by Barnes. The difference is due to our first-guess field being defined as a zonal average, annual mean, seasonal mean, or monthly mean for "all-data" climatologies, whereas Barnes used the first application of the analysis as a first-guess. Barnes (1964) also showed that applying the analysis scheme in an iterative fashion will result in convergence of the analyzed field to the observed data field. However, it is not desirable to approach the observed data too closely, because at least seven or eight gridpoints are needed to represent a Fourier component.

The response function given in (13) is useful in two ways: it is informative to know what Fourier components make up the analyses, and the computer programs used in generating the analyses can be checked for correctness by comparison with (13).

3.2.4. Choice of response function

The distribution of concurrently measured temperature and salinity observations (see appendix) at different depths and for the different averaging periods, are not regular in space or time. At one extreme, regions exist in which every one-degree square contains data and no interpolation needs to be performed. At the other extreme are regions in which few if any data exist. Thus, with variable data spacing the average separation distance between gridpoints containing data is a function of geographical position and averaging period. However, if we computed and used a different average separation distance for each variable at each depth and each averaging period, we would be generating analyses in which the wavelengths of observed phenomena might differ from one depth level to another and from one season to another. In WOA94, a fixed influence radius of 555 kilometers was used to allow uniformity in the analysis of all variables. For WOA98, WOA01, WOA05, WOA09, WOA13 and WOA18 analyses on the one-degree grid, a three-pass analysis based on Barnes (1964) with influence radii of 892, 669 and 446 km was used. For the WOA13 and WOA18 analyses on the quarter-degree grid, a three-pass analysis with radii of influence of 321, 267, and 214 km was used. (See Table 1 in section *3.4.1* for a comparison of the radii of influences on the different grids.)

Inspection of (3) shows that the difference between the analyzed field and the first-guess field values at any gridpoint is proportional to the sum of the weighted-differences between the observed mean and first-guess at all gridpoints containing data within the influence area.

The reason for using the five-point Shuman smoother and the median smoother is that our data are not evenly distributed in space. As the analysis moves from regions containing data to regions devoid of data, small-scale discontinuities may develop. The five-point Shuman and median smoothers are used to help eliminate these discontinuities. The five-point Shuman smoother does not affect the phase of the Fourier components that comprise an analyzed field.

The response functions for the analyses presented in these atlases are given in Table 5 and Figure 2. For comparison purposes, the

response function used by Levitus (1982), WOA94, and others are also presented. The response function represents the smoothing inherent in the objective analysis described above plus the effects of one application of the five-point Shuman smoother and one application of a five-point median smoother. The effect of varying the amount of smoothing in North Atlantic sea surface temperature (SST) fields has been quantified by Levitus (1982) for a particular case. In a region of strong SST gradient such as the Gulf Stream, the effect of smoothing can easily be responsible for differences between analyses exceeding 1.0°C.

To avoid the problem of the influence region extending across land or sills to adjacent basins, the objective analysis routine employs basin "identifiers" to preclude the use of data from adjacent basins. Table 6 lists these basins and the depth at which no exchange of information between basins is allowed during the objective analysis of data, *i.e.* "depths of mutual exclusion." Some regions are nearly, but not completely, isolated topographically. Because some of these nearly isolated basins have water mass properties that are different from surrounding basins, we have chosen to treat these as isolated basins as well. Not all such basins have been identified because of the complicated structure of the sea floor. In Table 6, a region marked with an asterisk (*) can interact with adjacent basins except for special areas such as the Isthmus of Panama.

3.2.5. First-guess field determination

There are gaps in the data coverage and, in some parts of the world ocean, there exist adjacent basins whose water mass properties are individually nearly homogeneous but have distinct basin-to-basin differences. Spurious features can be created when an influence area extends over two basins of this nature (basins are listed in Table 6). Our choice of first-guess field attempts to minimize the creation of such features. To maximize data coverage and best represent global variability, a set of "time-indeterminant" climatologies were produced as a first-guess for each set of decadal climatologies. The time-indeterminant climatologies used the first-guess field procedures developed for earlier versions of WOA: To provide a first-guess field for the "all-data" annual analysis at any standard level, we first zonally averaged the derived conductivity data in each one-degree latitude belt by individual ocean basins. The annual analysis was then used as the first-guess for each seasonal analysis and each seasonal analysis was used as a first-guess for the appropriate monthly analysis if computed. We should once again note, in the case for conductivity, the "all-data" analysis covers only the years 1978-2017 as this is the time period for which we are confident that most, if not all, salinity data is on the correct scale (PSS-78) and we are therefore able to accurately compute conductivity.

We then reanalyzed the conductivity data using the newly produced analyses as first-guess fields described as follows and as shown in Figure 3. A new annual mean was computed as the mean of the twelve monthly analyses for the upper 1500m, and the mean of the four seasons below 1500m depth. This new annual mean was used as the first-guess field for new seasonal analyses. These new seasonal analyses in turn were used to produce new monthly analyses. This procedure produces slightly smoother means.

These time-indeterminant monthly mean objectively analyzed conductivity fields were used as the first-guess fields for each "decadal" monthly climatology. Likewise, time-indeterminant seasonal and annual climatologies were used as first-guess fields for the seasonal and annual decadal climatologies.

We recognize that fairly large data-void

regions exist, in some cases to such an extent that a seasonal or monthly analysis in these regions is not meaningful. Geographic distribution of observations for the “all-data” annual periods (see appendices) is good for the upper layers of the ocean. By using an “all-data” annual mean, first-guess field regions where data exist for only one season or month will show no contribution to the annual cycle. By contrast, if we used a zonal average for each season or month, then, in those latitudes where gaps exist, the first-guess field would be heavily biased by the few data points that exist. If these were anomalous data in some way, an entire basin-wide belt might be affected.

One advantage of producing "global" fields for a particular compositing period (even though some regions are data void) is that such analyses can be modified by investigators for use in modeling studies.

For the quarter-degree first-guess field, the one-degree time-indeterminant field was also used. Each of the sixteen quarter-degree boxes enclosed used the one-degree time-indeterminant value as a first-guess, thereby projecting the one-degree climatology onto the quarter-degree grid. In those areas where there was no one-degree value due to land or bottom mask, the statistical mean for the entire basin at the given depth was used.

3.3. Choice of objective analysis procedures

Optimum interpolation (Gandin, 1963) has been used by some investigators to objectively analyze oceanographic data. We recognize the power of this technique but have not used it to produce analyzed fields. As described by Gandin (1963), optimum interpolation is used to analyze synoptic data using statistics based on historical data. In particular, second-order statistics such as correlation functions are used to estimate the distribution of first order parameters such as means. We attempt to map most fields in this atlas based on relatively sparse data sets.

Because of the paucity of data, we prefer not to use an analysis scheme that is based on second order statistics. In addition, as Gandin has noted, there are two limiting cases associated with optimum interpolation. The first is when a data distribution is dense. In this case, the choice of interpolation scheme makes little difference. The second case is when data are sparse. In this case, an analysis scheme based on second order statistics is of questionable value. For additional information on objective analysis procedures see Thiebaux and Pedder (1987) and Daley (1991).

3.4. Choice of spatial grid

The analyses that comprise WOA18 have been computed using the ETOPO2 land-sea topography to define ocean depths at each gridpoint (ETOPO2, 2006). From the ETOPO2 land mask, a quarter-degree land mask was created based on ocean bottom depth and land criteria. If sixteen or more 2-minute square values out of a possible forty-nine in a one-quarter-degree box were defined as land, then the quarter-degree gridbox was defined to be land. If no more than two of the 2-minute squares had the same depth value in a quarter-degree box, then the average value of the 2-minute ocean depths in that box was defined to be the depth of the quarter-degree gridbox. If ten or more 2-minute squares out of the forty-nine had a common bottom depth, then the depth of the quarter-degree box was set to the most common depth value. The same method was used to go from a quarter-degree to a one-degree resolution. In the one-degree resolution case, at least four points out of a possible sixteen (in a one-degree square) had to be land in order for the one-degree square to remain land and three out of sixteen had to have the same depth for the ocean depth to be set. These criteria yielded a mask that was

then modified by:

1. Connecting the Isthmus of Panama;
2. Maintaining an opening in the Straits of Gibraltar and in the English Channel;
3. Connecting the Kamchatka Peninsula and the Baja Peninsula to their respective continents.

The one-degree mask was created from the quarter-degree mask instead of directly from ETOPO2 in order to maintain consistency between the quarter-degree and one-degree masks.

3.4.1 Increased Spatial Resolution

WOA18 consists of temperature, salinity, density, and conductivity climatologies at both one-degree and quarter-degree spatial resolution.

example of this is the Gulf Stream. Figure 1 shows the 2005-2017 annual conductivity of the Gulf Stream at 0 m depth off of the Southeastern coast of the United States from WOA18. The quarter-degree resolution shows the tight conductivity gradient (related to the tight temperature gradient) of the Gulf Stream, whereas the one-degree resolution does not clearly define the Gulf Stream. The figure also depicts another improvement when moving from one-degree to quarter-degree resolution, and that is the ability to objectively analyze the physical variables closer to land. The quarter degree land gridboxes are closer and more confined to the coast than the one-degree land gridboxes, whose land gridboxes extend much further into the ocean. This allows the quarter-degree WOA18 to better use the large amount of data in near-shore observations.

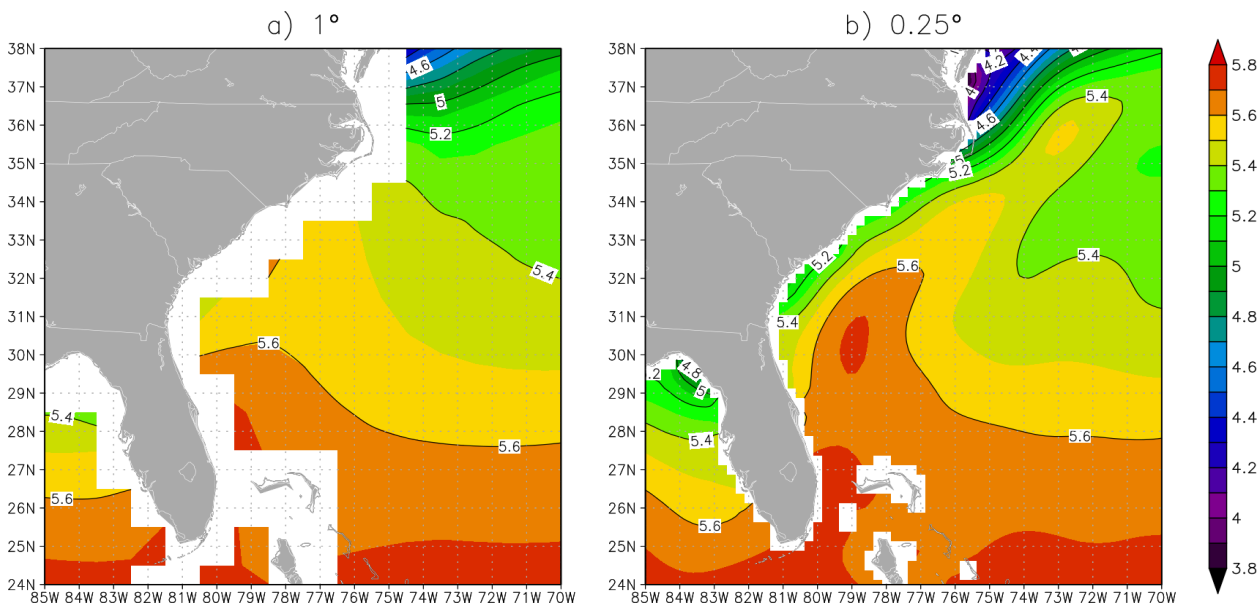

Figure 1. The annual conductivity of the Gulf Stream at 0 m depth for the 2005-2017 decade as represented by one-degree resolution and quarter-degree resolution.

The increase in spatial resolution from one-degree to quarter-degree between WOA09 and WOA13 (and WOA18) allowed regions whose features were not clearly defined in the one-degree analysis to be better represented in the higher-resolution analysis. An

Table 1. Radii of influence used in the objective analysis for the one-degree and quarter-degree climatologies.

Pass Number	1° Radius of Influence	1/4° Radius of Influence

1	892 km	321 km
2	669 km	267 km
3	446 km	214 km

However, some drawbacks are also encountered when moving to a higher resolution. The radius of influence used in the objective analysis is smaller in the quarter-degree grid as compared to the one-degree grid (see Table 1), thus in regions of very few observations, the analyzed value will not have many, if any, data points used in its calculation. This issue has been minimized somewhat by using the one-degree climatological products as first-guess fields for the quarter-degree products. For a full discussion of the methods used in producing the quarter-degree fields see Boyer *et al.* (2005).

4. RESULTS

The online figures for this atlas include seven types of horizontal maps representing annual, seasonal, and monthly spatial distribution of analyzed data and data statistics as a function of selected standard depth levels for conductivity:

a) Objectively analyzed conductivity climatology fields. One-degree or quarter-degree grids (as applicable) for which there were fewer than three values available in the objective analysis defined by the influence radius are denoted by a white "+" symbol.

b) Statistical mean conductivity fields. One-degree or quarter-degree grids for which there were fewer than three values available in the objective analysis defined by the influence radius are denoted by a white "+" symbol.

c) Data distribution fields of the number of conductivity observations in each one-degree or quarter-degree grid used in the objective analysis, binned into 1 to 2, 3-5, 6-10, 11-30, 31-50 and greater than 51 observations per grid square.

d) Standard deviation fields binned into several ranges depending on the depth level. The maximum value of the standard deviation is shown on the map.

e) Standard error of the mean fields binned into several ranges depending on the depth level.

f) Difference between observed and analyzed fields binned into several ranges depending on the depth level.

g) Difference between seasonal/monthly conductivity fields and the annual mean field.

h) The number of mean values within the radius of influence for each grid box was also calculated. This is not represented as stand-alone maps, but the results are used on a) and b) maps (as above) to shade the grid boxes with fewer than three mean values within the radius of influence. These calculations are available as data files online.

The maps are arranged by composite time periods: annual, seasonal, monthly. We note that the complete set of all climatological maps, objectively analyzed fields and associated statistical fields at all standard depth levels shown in Table 2 are available online. The complete set of data fields and documentation are available online as well. Table 7 describes all available conductivity maps and data fields.

All of the figures use consistent symbols and notations for displaying information. Continents are displayed as light-grey areas. Oceanic areas shallower than the standard depth level being displayed are shown as

solid gray areas. The objectively analyzed distribution fields include the nominal contour interval used. In addition, these maps may include in some cases additional contour lines displayed as dashed black lines. All of the maps were computer drafted using Generic Mapping Tools (GMT, Wessel and Smith, 1998).

We describe next the computation of annual and seasonal fields (section 4.1) and available objective and statistical fields (section 4.2).

4.1. Computation of annual and seasonal fields

After completion of all of our analyses we define a final annual analysis as the average of our twelve monthly mean fields in the upper 1500m of the ocean. Below 1500m depth we define an annual analysis as the mean of the four seasonal analyses. Our final seasonal analyses are defined as the average of the monthly analyses in the upper 1500m of the ocean.

4.2. Available statistical fields

Table 7 lists all objective and statistical fields calculated as part of WOA18. Climatologies of conductivity and associated statistics described in this document, as well as global figures of same can be obtained online.

The sample standard deviation in a gridbox was computed using:

$$s = \sqrt{\frac{\sum_{n=1}^{N}(x_n - \bar{x})^2}{N-1}} \qquad (14)$$

in which x_n= the nth data value in the gridbox, $\bar{x}$ = mean of all data values in the gridbox, and N = total number of data values in the gridbox. The standard error of the mean was computed by dividing the standard deviation by the square root of the number of observations in each gridbox.

In addition to statistical fields, the land/ocean bottom mask and basin definition mask are also available on the above-mentioned website. A user could take the standard depth level data from WOD18 with flags and these masks, and recreate the WOA18 fields following the procedures outlined in this document. Explanations and data formats for the data files are found under documentation on the WOA18 webpage.

4.3 Obtaining WOA18 fields online

The objective and statistical data fields can be obtained online in different digital formats at the WOA18 webpage. The WOA18 fields can be obtained in ASCII format (WOA native and comma-separated value [CSV]) and netCDF through our WOA18 webpage. For users interested in specific geographic areas, the World Ocean Atlas Select (WOAselect) selection tool can be used to designate a subset geographic area, depth, and oceanographic variable to view and optionally download climatological means or related statistics in shapefile format which is compatible with GIS software such as ESRI ArcMap. WOA18 includes a digital collection of "JPEG" images of the objective and statistical fields. In addition, WOA18 can be obtained in Ocean Data View (ODV) format. WOA18 will be available through other online locations as well. WOA98, WOA01, WOA05, WOA09 and WOA13 are presently served through the IRI/LDEO Climate Data Library with access to statistical and objectively analyzed fields in a variety of digital formats.

5. SUMMARY

In the preceding sections we have described the results of a project to objectively analyze all historically derived (from in situ temperature and salinity profiles) conductivity data in WOD18. We desire to build a set of climatological analyses that are

identical in all respects for all variables including relatively data sparse variables such as nutrients. This provides investigators with a consistent set of analyses to use.

One advantage of the analysis techniques used in this atlas is that we know the amount of smoothing by objective analyses as given by the response function in Table 5 and Figure 2. We believe this to be an important function for constructing and describing a climatology of any geophysical parameter. Particularly when computing anomalies from a standard climatology, it is important that the synoptic field be smoothed to the same extent as the climatology to prevent generation of spurious anomalies simply through differences in smoothing. A second reason is that purely diagnostic computations require a minimum of seven or eight gridpoints to represent any Fourier component with accuracy. Higher order derivatives will require more smoothing.

We have attempted to create objectively analyzed fields and data sets that can be used as a "black box." We emphasize that some quality control procedures used are subjective. For those users who wish to make their own choices, all the data used in our analyses are available both at standard depth levels as well as observed depth levels. The results presented in this atlas show some features that are suspect and may be due to non-representative data that were not flagged by the quality control techniques used. Although we have attempted to eliminate as many of these features as possible by flagging the data which generate these features, some obviously could remain. Some may eventually turn out not to be artifacts but rather to represent real features, not yet capable of being described in a meaningful way due to lack of data.

6. FUTURE WORK

Our analyses will be updated when justified by additional observations. As more data are received at NCEI/WDC, we will also be able to produce improved higher resolution climatologies for conductivity.

7. REFERENCES

Achtemeier, G.L. (1987). On the concept of varying influence radii for a successive corrections objective analysis. *Mon. Wea. Rev.,* 11, 1761-1771.

Antonov, J.I., S. Levitus, T.P. Boyer, M.E. Conkright, T.D. O'Brien, and C. Stephens (1998a). World Ocean Atlas 1998. Vol. 1: Temperature of the Atlantic Ocean. *NOAA Atlas NESDIS 27*, U.S. Government Printing Office, Washington, D.C., 166 pp.

Antonov, J.I., S. Levitus, T.P. Boyer, M.E. Conkright, T.D. O'Brien, and C. Stephens (1998b). World Ocean Atlas 1998. Vol. 2: Temperature of the Pacific Ocean. *NOAA Atlas NESDIS 28*, U.S. Government Printing Office, Washington, D.C., 166 pp.

Antonov, J.I., S. Levitus, T.P. Boyer, M.E. Conkright, T.D. O'Brien, C. Stephens, and B. Trotsenko (1998c). World Ocean Atlas 1998. Vol. 3: Temperature of the Indian Ocean. *NOAA Atlas NESDIS 29*, U.S. Government Printing Office, Washington, D.C., 166 pp.

Antonov, J.I., R.A. Locarnini, T.P. Boyer, H.E. Garcia, and A.V. Mishonov (2006). World Ocean Atlas 2005. Vol. 2: Salinity. S. Levitus, Ed. *NOAA Atlas NESDIS 62*, U.S. Government Printing Office, Washington, D.C., 182 pp.

Antonov, J.I., D. Seidov, T.P. Boyer, R.A. Locarnini, A.V. Mishonov, H.E. Garcia, O.K. Baranova, M.M. Zweng, and D.R. Johnson (2010). World Ocean Atlas 2009. Vol. 2: Salinity. S. Levitus, Ed. *NOAA Atlas NESDIS 69*, U.S. Government Printing Office, Washington, D.C., 184 pp.

Barnes, S.L. (1964). A technique for maximizing details in numerical weather map analysis. *J. App. Meteor.*, 3, 396-409.

Barnes, S.L. (1973). Mesoscale objective map analysis using weighted time series observations. *NOAA Technical Memorandum ERL* NSSL-62, 60 pp.

Barnes, S.L. (1994). Applications of the Barnes Objective Analysis Scheme, Part III: Tuning for Minimum Error. *J. Atmos. Oceanic Technol.,* 11, 1459-1479.

Bergthorsson, P. and B. Doos, 1955. Numerical Weather map analysis. *Tellus*, 7, 329-340.

Boyer, T.P. and S. Levitus (1994). Quality control and processing of historical temperature, salinity and

oxygen data. *NOAA Technical Report NESDIS 81*, 65 pp.

Boyer, T.P., S. Levitus, J.I. Antonov, M.E. Conkright, T.D. O'Brien, and C. Stephens (1998a). World Ocean Atlas 1998. Vol. 4: Salinity of the Atlantic Ocean. *NOAA Atlas NESDIS* 30, U.S. Government Printing Office, Washington, D.C., 166 pp.

Boyer, T.P., S. Levitus, J.I. Antonov, M.E. Conkright, T.D. O'Brien, and C. Stephens (1998b). World Ocean Atlas 1998. Vol. 5: Salinity of the Pacific Ocean. *NOAA Atlas NESDIS 31*, U.S. Government Printing Office, Washington, D.C., 166 pp.

Boyer, T.P., S. Levitus, J.I. Antonov, M.E. Conkright, T.D. O'Brien, C. Stephens, and B. Trotsenko (1998c). World Ocean Atlas 1998. Vol. 6: Salinity of the Indian Ocean. *NOAA Atlas NESDIS 32*, U.S. Government Printing Office, Washington, D.C., 166 pp.

Boyer, T.P., C. Stephens, J.I. Antonov, M.E. Conkright, R.A. Locarnini, T.D. O'Brien, and H.E. Garcia (2002). World Ocean Atlas 2001. Vol. 2: Salinity. S. Levitus, Ed., *NOAA Atlas NESDIS 50*, U.S. Government Printing Office, Washington, D.C., 165 pp.

Boyer, T.P, S. Levitus, H.E. Garcia, R.A. Locarnini, C. Stephens, J.I. Antonov (2005). Objective analyses of annual, seasonal, and monthly temperature and salinity for the world ocean on a ¼ degree grid. *International Journal of Climatology*, 25, 931-945.

Boyer, T.P., J.I. Antonov, O.K. Baranova, C. Coleman, H.E. Garcia, A. Grodsky, D.R. Johnson, T.D. O'Brien, C.R. Paver, R.A. Locarnini, A.V. Mishonov, J.R. Reagan, D. Seidov, I.V. Smolyar, and M.M. Zweng (2013). World Ocean Database 2013. S. Levitus, Ed., A. Mishonov Tech. Ed., *NOAA Atlas NESDIS 72*, 209 pp.

Boyer, T.P., R.A. Locarnini, M.M. Zweng, A.V. Mishonov, J.R. Reagan, J.I. Antonov, H.E. Garcia, O.K. Baranova, D.R. Johnson, D. Seidov, M.M. Biddle, M. Hamilton (2015). *Changes to calculations of the World Ocean Atlas 2013 for ver.2*. http://data.nodc.noaa.gov/woa/WOA13/DOC/woa13v2_changes.pdf.

Boyer, T.P., O.K. Baranova, C. Coleman, H.E. Garcia, A. Grodsky, R.A. Locarnini, A.V. Mishonov, C.R. Paver, J.R. Reagan, D. Seidov, I.V. Smolyar, K.W. Weathers, M.M. Zweng (2019). World Ocean Database 2018. A. V. Mishonov, Technical Editor, NOAA Atlas NESDIS 87.

Conkright, M.E., S. Levitus, and T.P. Boyer (1994). World Ocean Atlas 1994. Vol. 1: Nutrients. *NOAA Atlas NESDIS 1*, U.S. Government Printing Office, Washington, D.C., 150 pp.

Conkright, M.E., T.D. O'Brien, S. Levitus, T.P. Boyer, J.I. Antonov, and C. Stephens (1998a). World Ocean Atlas 1998. Vol. 10: Nutrients and Chlorophyll of the Atlantic Ocean. *NOAA Atlas NESDIS 36*, U.S. Government Printing Office, Washington, D.C., 245 pp.

Conkright, M.E., T.D. O'Brien, S. Levitus, T.P. Boyer, J.I. Antonov, and C. Stephens (1998b). World Ocean Atlas 1998. Vol. 11: Nutrients and Chlorophyll of the Pacific Ocean. *NOAA Atlas NESDIS 37*, U.S. Government Printing Office, Washington, D.C., 245 pp.

Conkright, M.E., T.D. O'Brien, S. Levitus, T.P. Boyer, J.I. Antonov, and C. Stephens (1998c). World Ocean Atlas 1998. Vol. 12: Nutrients and Chlorophyll of the Indian Ocean. *NOAA Atlas NESDIS 38*, U.S. Government Printing Office, Washington, D.C., 245 pp.

Conkright, M.E., H.E. Garcia, T.D. O'Brien, R.A. Locarnini, T.P. Boyer, C. Stephens, and J.I. Antonov (2002). World Ocean Atlas 2001. Vol. 4: Nutrients. S. Levitus, Ed., *NOAA Atlas NESDIS 52*, U.S. Government Printing Office, Washington, D.C., 392 pp.

Cressman, G.P. (1959). An operational objective analysis scheme. *Mon. Wea. Rev.*, 87, 329-340.

Daley, R. (1991). *Atmospheric Data Analysis.* Cambridge University Press, Cambridge, 457 pp.

ETOPO2 (2006). Data Announcements 06-MGG-01, 2-Minute Gridded Global Relief Data. NOAA, *National Geophysical Data Center*, Boulder, CO.

Gandin, L.S. (1963). Objective Analysis of Meteorological fields. *Gidromet Izdat*, Leningrad (translation by Israel program for Scientific Translations), Jerusalem, 1966, 242 pp.

Garcia, H.E., R.A. Locarnini, T.P. Boyer, and J.I. Antonov (2006a). World Ocean Atlas 2005. Vol. 3: Dissolved Oxygen, Apparent Oxygen Utilization, and Oxygen Saturation. S. Levitus, Ed. *NOAA Atlas NESDIS 63*, U.S. Government Printing Office, Washington, D.C., 342 pp.

Garcia H.E., R.A. Locarnini, T.P. Boyer, and J.I. Antonov (2006b). World Ocean Atlas 2005. Vol. 4: Nutrients (phosphate, nitrate, silicate), S. Levitus, Ed., *NOAA Atlas NESDIS 64*, U.S. Government Printing Office, Washington, D.C., 395 pp.

Garcia, H.E., R.A. Locarnini, T.P. Boyer, and J.I. Antonov (2010a). World Ocean Atlas 2009, Vol. 3: Dissolved Oxygen, Apparent Oxygen Utilization, and Oxygen Saturation. S. Levitus, Ed. *NOAA Atlas NESDIS 70*, U.S. Government Printing Office, Washington, D.C., 344 pp.

Garcia, H.E., R.A. Locarnini, T.P. Boyer, and J.I.

Antonov (2010b). World Ocean Atlas 2009. *I* S. Levitus, Ed. *NOAA Atlas NESDIS 71*, U.S. Government Printing Office, Washington, D.C., 398 pp.

Garcia H.E., T.P. Boyer, R.A. Locarnini, A.V. Mishonov, J.I. Antonov, O.K. Baranova, M.M. Zweng, J.R. Reagan, D.R. Johnson (2013a). World Ocean Atlas 2013, Vol. 3: Oxygen. S. Levitus, Ed.; A. Mishonov, Tech. Ed. *NOAA Atlas NESDIS 75*.

Garcia H.E., T.P. Boyer, R.A. Locarnini, A.V. Mishonov, J.I. Antonov, O.K. Baranova, M.M. Zweng, J.R. Reagan, D.R. Johnson (2013b). World Ocean Atlas 2013, Vol. 4: Nutrients. S. Levitus, Ed.; A. Mishonov, Tech. Ed. *NOAA Atlas NESDIS 76*.

Garcia, H. E., K. Weathers, C. R. Paver, I. Smolyar, T. P. Boyer, R. A. Locarnini, M. M. Zweng, A. V. Mishonov, O. K. Baranova, D. Seidov, and J. R. Reagan (2019a). *World Ocean Atlas 2018, Volume 3: Dissolved Oxygen, Apparent Oxygen Utilization, and Oxygen Saturation.* A. Mishonov Technical Ed.; NOAA Atlas NESDIS 83, 38 pp.

Garcia, H. E., K. Weathers, C. R. Paver, I. Smolyar, T. P. Boyer, R. A. Locarnini, M. M. Zweng, A. V. Mishonov, O. K. Baranova, D. Seidov, and J. R. Reagan (2019b). *World Ocean Atlas 2018, Volume 4: Dissolved Inorganic Nutrients (phosphate, nitrate and nitrate+nitrite, silicate).* A. Mishonov Technical Ed.; NOAA Atlas NESDIS 84, 35 pp.

Garcia, H. E., T. P. Boyer, R. A. Locarnini, O. K. Baranova, M. M. Zweng (2019). World Ocean Database 2018: User's Manual (prerelease). A.V. Mishonov, Technical Ed., NOAA, Silver Spring, MD.

Hesselberg, T. and H.U. Sverdrup (1914). Die Stabilitutsverhaltnisse des Seewassers bei Vertitalen Verschiebungen. *Aarb. Bergen Mus.,* No. 14, 17 pp.

Hill, K.D., T. Dauphinee, D.J. Woods (1986). The extension of the practical salinity scale 1978 to low salinities. *IEEE J Ocean Eng.* 11(1), pp. 109–112.

IOC (1998). Global Temperature-Salinity Profile Programme (GTSPP) – Overview and Future. *IOC Technical Series, 49*, Intergovernmental Oceanographic Commission, Paris, 12 pp.

IOC, SCOR and IAPSO (2010). The international thermodynamic equation of seawater – 2010: Calculation and use of thermodynamic properties. Intergovernmental Oceanographic Commission, Manuals and Guides No. 56, UNESCO, 196 pp. Available from http://www.teos-10.org/

Irrgang, C., J. Saynisch and M. Thomas (2019). Estimating global ocean heat content from tidal magnetic satellite observations. *Scientific Reports,* 9**,** 7893.

Jackett, D.R. and T.J. McDougall (1995). Minimal Adjustment of Hydrographic Profiles to Achieve Static Stability. *J. Atmos. Oceanic Technol.*, 12, 381-389.

JPOTS (Joint Panel on Oceanographic Tables and Standards) Editorial Panel (1991). Processing of Oceanographic Station Data. *UNESCO*, Paris, 138 pp.

Johnson, D.R., T.P. Boyer, H.E. Garcia, R.A. Locarnini, O.K. Baranova, and M.M. Zweng (2013). World Ocean Database 2013 User's Manual. S. Levitus, Ed., A. Mishonov, Tech. Ed. *NODC Internal Report 22*, U.S. Government Printing Office, Washington, D.C., 172 pp.

Johnson, G.C. (1995). Revised XCTD fall-rate equation coefficients from CTD data. *J. Atmos. Oceanic Technol.*, 12, 1367-1373.

Kizu, S., H. Onishi, T. Suga, K. Hanawa, T. Watanabe, and H. Iwamiya (2008). Evaluation of the fall rates of the present and developmental XCTDs. *Deep-Sea Res. I*, 55,571–586.

Koso, Y., H. Ishii, and M. Fujita (2005). An examination of the depth conversion formula of XCTD-2F. *Technical Bulletin on Hydrology and Oceanography*, 23, 93–98 (in Japanese).

Levitus, S. (1982). Climatological Atlas of the World Ocean. *NOAA Professional Paper No. 13*, U.S. Government Printing Office, Washington, D.C., 173 pp.

Levitus, S. and T.P. Boyer (1994a). World Ocean Atlas 1994. Vol. 2: Oxygen. *NOAA Atlas NESDIS 2*, U.S. Government Printing Office, Washington, D.C., 186 pp.

Levitus, S. and T.P. Boyer (1994b). World Ocean Atlas 1994. Vol. 4: Temperature. *NOAA Atlas NESDIS 4*, U.S. Government Printing Office, Wash., D.C., 117 pp.

Levitus, S. and G. Isayev (1992). A polynomial approximation to the International Equation of State for Seawater. *J. Atmos. Oceanic Technol.,* 9, 705-708.

Levitus, S., R. Burgett, T.P. Boyer (1994). World Ocean Atlas 1994, Vol. 3: Salinity. *NOAA Atlas NESDIS 3*, U.S. Government Printing Office, Washington, D.C., 99 pp.

Levitus, S., S. Sato, C. Maillard, N. Mikhailov, P. Caldwell, and H. Dooley (2005). Building Ocean Profile-Plankton Databases for Climate and Ecosystem Research, *NOAA Technical Report NESDIS 117*, U.S Government Printing Office, Washington, D.C., 29 pp.

Locarnini, R.A., T.D. O'Brien, H.E. Garcia, J.I.

Antonov, T.P. Boyer, M.E. Conkright, and C. Stephens (2002). World Ocean Atlas 2001. Vol. 3: Oxygen. S. Levitus, Ed., *NOAA Atlas NESDIS 51*, U.S. Government Printing Office, Washington, D.C., 286 pp.

Locarnini, R.A., A.V. Mishonov, J.I. Antonov, T.P. Boyer, and H.E. Garcia (2006). World Ocean Atlas 2005. Vol. 1: Temperature. S. Levitus, Ed., NOAA *Atlas NESDIS 61*, U.S. Government Printing Office, Washington, D.C. 182 pp.

Locarnini, R.A., A.V. Mishonov, J.I. Antonov, T.P. Boyer, and H.E. Garcia (2010). World Ocean Atlas 2009. Vol. 1: Temperature. S. Levitus, Ed. *NOAA Atlas NESDIS 68*, U.S. Government Printing Office, Washington, D.C., 184 pp.

Locarnini, R.A., A.V. Mishonov, J.I. Antonov, T.P. Boyer, H.E. Garcia, O.K. Baranova, M.M. Zweng, C.R. Paver, J.R. Reagan, D.R. Johnson, M. Hamilton, D. Seidov (2013). World Ocean Atlas 2013, Vol. 1: Temperature. S. Levitus, Ed. A. Mishonov, Tech. Ed. *NOAA Atlas NESDIS 73*, 40 pp.

Locarnini, R. A., A. V. Mishonov, O. K. Baranova, T. P. Boyer, M. M. Zweng, H. E. Garcia, J. R. Reagan, D. Seidov, K. Weathers, C. R. Paver, and I. Smolyar (2019). *World Ocean Atlas 2018, Volume 1: Temperature.* A. Mishonov Technical Ed.; NOAA Atlas NESDIS 81, 52 pp.

Lynn, R. J. (1967). Seasonal variations of temperature and salinity at 10 meters in the California Current, *CalCOFI Reports*, 11, 157-174.

Lynn, R.J. and J.L. Reid (1968). Characteristics and circulation of deep and abyssal waters. *Deep-Sea Res.*, 15, 577-598.

McDougall, T.J. and P.M. Barker (2011). Getting started with TEOS-10 and the Gibbs Seawater (GSW) Oceanographic Toolbox, SCOR/IAPSO WG127, ISBN 978-0-646-55621-5, 28pp.

Mizuno, K. and T. Watanabe (1998). Preliminary results of in-situ XCTD/CTD comparison test. *J. Oceanogr.*, 54(4), 373-380.

Neumann, G. and W.J. Pierson (1966). Principles of Physical Oceanography. *Prentice Hall Inc.*, Englewood Cliffs, N.J., 545 pp.

O'Brien, T.D., S. Levitus, T.P. Boyer, M.E. Conkright, J.I. Antonov, and C. Stephens (1998a). World Ocean Atlas 1998. Vol. 7: Oxygen of the Atlantic Ocean. *NOAA Atlas NESDIS 33*, U.S. Government Printing Office, Washington, D.C., 234 pp.

O'Brien, T.D., S. Levitus, T.P. Boyer, M.E. Conkright, J.I. Antonov, and C. Stephens (1998b). World Ocean Atlas 1998. Vol. 8: Oxygen of the Pacific Ocean. *NOAA Atlas NESDIS 34*, U.S. Government Printing Office, Washington, D.C., pp.

O'Brien, T.D., S. Levitus, T.P. Boyer, M.E. Conkright, J.I. Antonov, and C. Stephens (1998c). World Ocean Atlas 1998. Vol. 9: Oxygen of the Indian Ocean. *NOAA Atlas NESDIS 35*, U.S. Government Printing Office, Washington, D.C., 234 pp.

Rabiner, L.R., M.R. Sambur, and C.E. Schmidt (1975). Applications of a nonlinear smoothing algorithm to speech processing*, IEEE Trans. on Acoustics, Speech and Signal Processing*, 23, 552-557.

Reiniger, R.F. and C.F. Ross (1968). A method of interpolation with application to oceanographic data. *Deep-Sea Res.*, 9, 185-193.

Sasaki, Y. (1960). An objective analysis for determining initial conditions for the primitive equations. Ref. 60-1 6T, Atmospheric Research Lab., *Univ. of Oklahoma Research Institute*, Norman, 23 pp.

Seaman, R.S. (1983). Objective Analysis accuracies of statistical interpolation and successive correction schemes. *Australian Meteor. Mag.*, 31, 225-240.

Seidov, D., A. Mishonov, J. Reagan, O. Baranova, S. Cross, and R. Parsons (2018). Regional climatology of the Northwest Atlantic Ocean—high-resolution mapping of ocean structure and change, *Bulletin of the American Meteorological Society*, 9(10), doi:10.1175/BAMS-D-17-0205.1.

Shuman, F.G. (1957). Numerical methods in weather prediction: II. Smoothing and filtering. *Mon. Wea. Rev.*, 85, 357-361.

Smith, D.R., and F.Leslie (1984). Error determination of a successive correction type objective analysis scheme. *J. Atmos. Oceanic Technol.*, 1, 121-130.

Smith, D.R., M.E. Pumphry, and J.T. Snow (1986). A comparison of errors in objectively analyzed fields for uniform and nonuniform station distribution, *J. Atmos. Oceanic Technol.*, 3, 84-97.

Stephens, C., J.I. Antonov, T.P. Boyer, M.E. Conkright, R.A. Locarnini, T.D. O'Brien, H.E. Garcia (2002). World Ocean Atlas 2001. Vol. 1: Temperature. S. Levitus, Ed., *NOAA Atlas NESDIS 49*, U.S. Government Printing Office, Washington, D.C., 167 pp.

Sverdrup, H.U., M.W. Johnson, and R.H. Fleming (1942). The Oceans: Their physics, chemistry, and general biology. *Prentice Hall*, 1060 pp.

Thiebaux, H.J. and M.A. Pedder (1987). Spatial Objective Analysis: with applications in atmospheric science. *Academic Press*, 299 pp.

Trossman, D.S. and R.H. Tyler (2019). Predictability of ocean heat content from electrical conductance. *Journal of Geophysical Research – Oceans,* 124(1)**,** 667–679.

Tukey, J.W. (1974). Nonlinear (nonsuperposable)

methods for smoothing data, in *"Cong. Rec."*, 1974 *EASCON*, 673 pp.

Tyler, R.H. and T.J. Sabaka (2016). Magnetic remote sensing of ocean heat content. AGU Fall Meeting 2016, abstract #GC31D-1142.

Tyler, R. H., T. P. Boyer, T. Minami, M. M. Zweng, and J. R. Reagan (2017). Electrical conductivity of the global ocean. *Earth, Planets and Space*, 69**:**156, doi:10.1186/s40623-017-0739-7.

Wessel, P. and W.H.F. Smith (1998). New, improved version of Generic Mapping Tools released, *EOS Trans. Amer. Geophys. U.*, 79, 579.

Zweng, M. M., J. R. Reagan, D. Seidov, T. P. Boyer, R. A. Locarnini, H. E. Garcia, A. V. Mishonov, O. K. Baranova, K. Weathers, C. R. Paver, and I. Smolyar (2019). *World Ocean Atlas 2018, Volume 2: Salinity.* A. Mishonov Technical Ed.; NOAA Atlas NESDIS 82, 50 pp.

Table 2. Descriptions of climatologies for conductivity. The standard depth levels are shown in Table 4.

Oceanographic variable	Depths for annual climatology	Depths for seasonal climatology	Depths for monthly climatology	Datasets used to calculate climatology
Conductivity	0-5500 meters (102 levels)	0-5500 meters (102 levels)	0-1500 meters (57 levels)	OSD, CTD, MRB, PFL, DRB, UOR, SUR, GLD

Table 3. Descriptions of datasets in WOD18.

OSD	Bottle, low-resolution Conductivity-Temperature-Depth (CTD), low-resolution XCTD data, and plankton data
CTD	High-resolution Conductivity-Temperature-Depth (CTD) data and high-resolution XCTD data
MBT	Mechanical Bathythermograph (MBT) data, DBT, micro-BT
XBT	Expendable Bathythermograph (XBT) data
SUR	Surface only data (bucket, thermosalinograph)
APB	Autonomous Pinniped Bathythermograph - Time-Temperature-Depth recorders attached to elephant seals
MRB	Moored buoy data from TAO (Tropical Atmosphere-Ocean), PIRATA (moored array in the tropical Atlantic), TRITON (Japan-JAMSTEC), RAMA (moored array in the tropical Indian) and individual (usually coastal) buoys.
PFL	Profiling float data
DRB	Drifting buoy data from surface drifting buoys with thermistor chains
UOR	Undulating Oceanographic Recorder data from a Conductivity/Temperature/Depth probe mounted on a towed undulating vehicle
GLD	Glider data

Table 4. Acceptable distances (m) for defining interior (A) and exterior (B) values used in the Reiniger-Ross scheme for interpolating observed level data to standard levels.

Standard Level #	Standard Depths (m)	A	B	Standard Level #	Standard Depths (m)	A	B
1	0	50	200	52	1250	200	400
2	5	50	200	53	1300	200	1000
3	10	50	200	54	1350	200	1000
4	15	50	200	55	1400	200	1000
5	20	50	200	56	1450	200	1000
6	25	50	200	57	1500	200	1000
7	30	50	200	58	1550	200	1000
8	35	50	200	59	1600	200	1000
9	40	50	200	60	1650	200	1000
10	45	50	200	61	1700	200	1000
11	50	50	200	62	1750	200	1000
12	55	50	200	63	1800	200	1000
13	60	50	200	64	1850	200	1000
14	65	50	200	65	1900	200	1000
15	70	50	200	66	1950	200	1000
16	75	50	200	67	2000	1000	1000
17	80	50	200	68	2100	1000	1000
18	85	50	200	69	2200	1000	1000
19	90	50	200	70	2300	1000	1000
20	95	50	200	71	2400	1000	1000
21	100	50	200	72	2500	1000	1000
22	125	50	200	73	2600	1000	1000
23	150	50	200	74	2700	1000	1000
24	175	50	200	75	2800	1000	1000
25	200	50	200	76	2900	1000	1000
26	225	50	200	77	3000	1000	1000
27	250	100	200	78	3100	1000	1000
28	275	100	200	79	3200	1000	1000
29	300	100	200	80	3300	1000	1000
30	325	100	200	81	3400	1000	1000
31	350	100	200	82	3500	1000	1000
32	375	100	200	83	3600	1000	1000
33	400	100	200	84	3700	1000	1000

Standard Level #	Standard Depths (m)	A	B	Standard Level #	Standard Depths (m)	A	B
34	425	100	200	85	3800	1000	1000
35	450	100	200	86	3900	1000	1000
36	475	100	200	87	4000	1000	1000
37	500	100	400	88	4100	1000	1000
38	550	100	400	89	4200	1000	1000
39	600	100	400	90	4300	1000	1000
40	650	100	400	91	4400	1000	1000
41	700	100	400	92	4500	1000	1000
42	750	100	400	93	4600	1000	1000
43	800	100	400	94	4700	1000	1000
44	850	100	400	95	4800	1000	1000
45	900	200	400	96	4900	1000	1000
46	950	200	400	97	5000	1000	1000
47	1000	200	400	98	5100	1000	1000
48	1050	200	400	99	5200	1000	1000
49	1100	200	400	100	5300	1000	1000
50	1150	200	400	101	5400	1000	1000
51	1200	200	400	102	5500	1000	1000

Table 5. Response function of the objective analysis scheme as a function of wavelength for WOA18 and earlier analyses. Response function is normalized to 1.0.

Wavelength[1]	Levitus (1982)	WOA94	WOA98, '01, '05, '09, '13 One-degree	WOA13 Quarter-degree
360ΔX	1.000	0.999	1.000	1.000
180ΔX	1.000	0.997	0.999	1.000
120ΔX	1.000	0.994	0.999	0.999
90ΔX	1.000	0.989	0.998	0.999
72ΔX	1.000	0.983	0.997	0.998
60ΔX	1.000	0.976	0.995	0.997
45ΔX	1.000	0.957	0.992	0.996
40ΔX	0.999	0.946	0.990	0.994
36ΔX	0.999	0.934	0.987	0.993
30ΔX	0.996	0.907	0.981	0.990
24ΔX	0.983	0.857	0.969	0.984
20ΔX	0.955	0.801	0.952	0.978
18ΔX	0.923	0.759	0.937	0.972
15ΔX	0.828	0.671	0.898	0.960
12ΔX	0.626	0.532	0.813	0.939
10ΔX	0.417	0.397	0.698	0.913
9ΔX	0.299	0.315	0.611	0.894
8ΔX	0.186	0.226	0.500	0.868
6ΔX	3.75×10^{-2}	0.059	0.229	0.777
5ΔX	1.34×10^{-2}	0.019	0.105	0.695
4ΔX	1.32×10^{-3}	2.23×10^{-3}	2.75×10^{-2}	0.567
3ΔX	2.51×10^{-3}	1.90×10^{-4}	5.41×10^{-3}	0.364
2ΔX	5.61×10^{-7}	5.30×10^{-7}	1.36×10^{-6}	0.103
1ΔX	N/A	N/A	N/A	1.13×10^{-4}

[1] For ΔX = 111 km, the meridional separation at the Equator.

Table 6. Basins defined for objective analysis and the shallowest standard depth level for which each basin is defined.

#	Basin[1]	Standard Depth Level	#	Basin[1]	Standard Depth Level
1	Atlantic Ocean	1*	30	North American Basin	82
2	Pacific Ocean	1*	31	West European Basin	82
3	Indian Ocean	1*	32	Southeast Indian Basin	82
4	Mediterranean Sea	1*	33	Coral Sea	82
5	Baltic Sea	1	34	East Indian Basin	82
6	Black Sea	1	35	Central Indian Basin	82
7	Red Sea	1	36	Southwest Atlantic Basin	82
8	Persian Gulf	1	37	Southeast Atlantic Basin	82
9	Hudson Bay	1	38	Southeast Pacific Basin	82
10	Southern Ocean	1*	39	Guatemala Basin	82
11	Arctic Ocean	1	40	East Caroline Basin	87
12	Sea of Japan	1	41	Marianas Basin	87
13	Kara Sea	22	42	Philippine Sea	87
14	Sulu Sea	25	43	Arabian Sea	87
15	Baffin Bay	37	44	Chile Basin	87
16	East Mediterranean	41	45	Somali Basin	87
17	West Mediterranean	47	46	Mascarene Basin	87
18	Sea of Okhotsk	47	47	Crozet Basin	87
19	Banda Sea	55	48	Guinea Basin	87
20	Caribbean Sea	55	49	Brazil Basin	92
21	Andaman Basin	62	50	Argentine Basin	92
22	North Caribbean	67	51	Tasman Sea	87
23	Gulf of Mexico	67	52	Atlantic Indian Basin	92
24	Beaufort Sea	77	53	Caspian Sea	1
25	South China Sea	77	54	Sulu Sea II	37
26	Barents Sea	77	55	Venezuela Basin	37
27	Celebes Sea	62	56	Bay of Bengal	1*
28	Aleutian Basin	77	57	Java Sea	16
29	Fiji Basin	82	58	East Indian Atlantic Basin	97

[1] Basins marked with a "*" can interact with adjacent basins in the objective analysis.

Table 7. Statistical fields calculated as part of WOA18 Conductivity

(√ denotes fields were calculated and are publicly available).

Statistical Field	One Degree Fields Calculated	Quarter Degree Fields Calculated	Five Degree Statistics Calculated
Objectively Analyzed Climatology – Annual[1]	√	√	
Objectively Analyzed Climatology - Seasonal[1]	√	√	
Objectively Analyzed Climatology - Monthly[1]	√	√	
Statistical Mean[1,2]	√	√	√
Number Of Observations[1]	√	√	√
Seasonal (Monthly) Climatology Minus Annual Climatology[1]	√	√	
Standard Deviation From Statistical Mean[1,2]	√	√	√
Standard Error Of The Statistical Mean[1,2]	√	√	√
Statistical Mean Minus Objectively Analyzed Climatology[1,2]	√	√	
Number Of Mean Values Within Radius Of Influence[1]	√	√	

[1] Conductivity climatologies are available only for the "climate normal" decadal average (1981-2010) and the 2005-2017 decade.
[2] Statistical fields are only available when the objectively analyzed fields are available (for one- and quarter-degree fields).

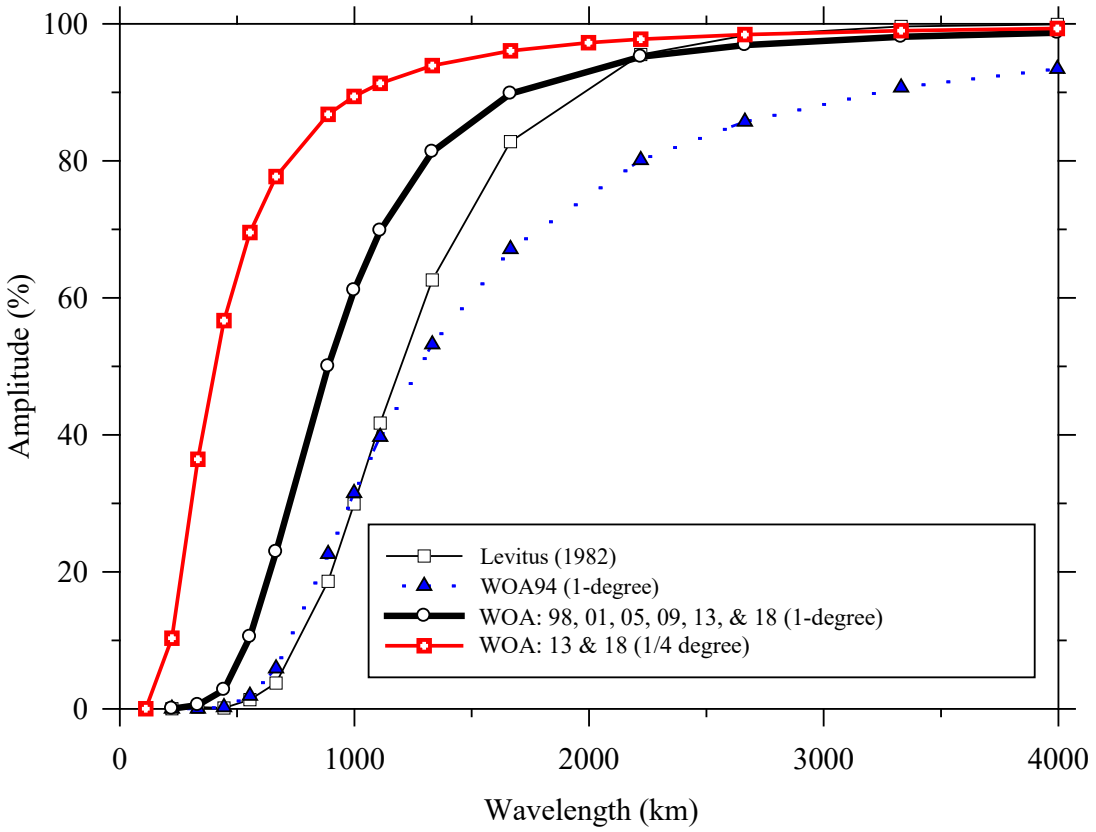

Figure 2. Response function of the WOA18, WOA13, WOA09, WOA05, WOA01, WOA98, WOA94, and Levitus (1982) objective analysis schemes.

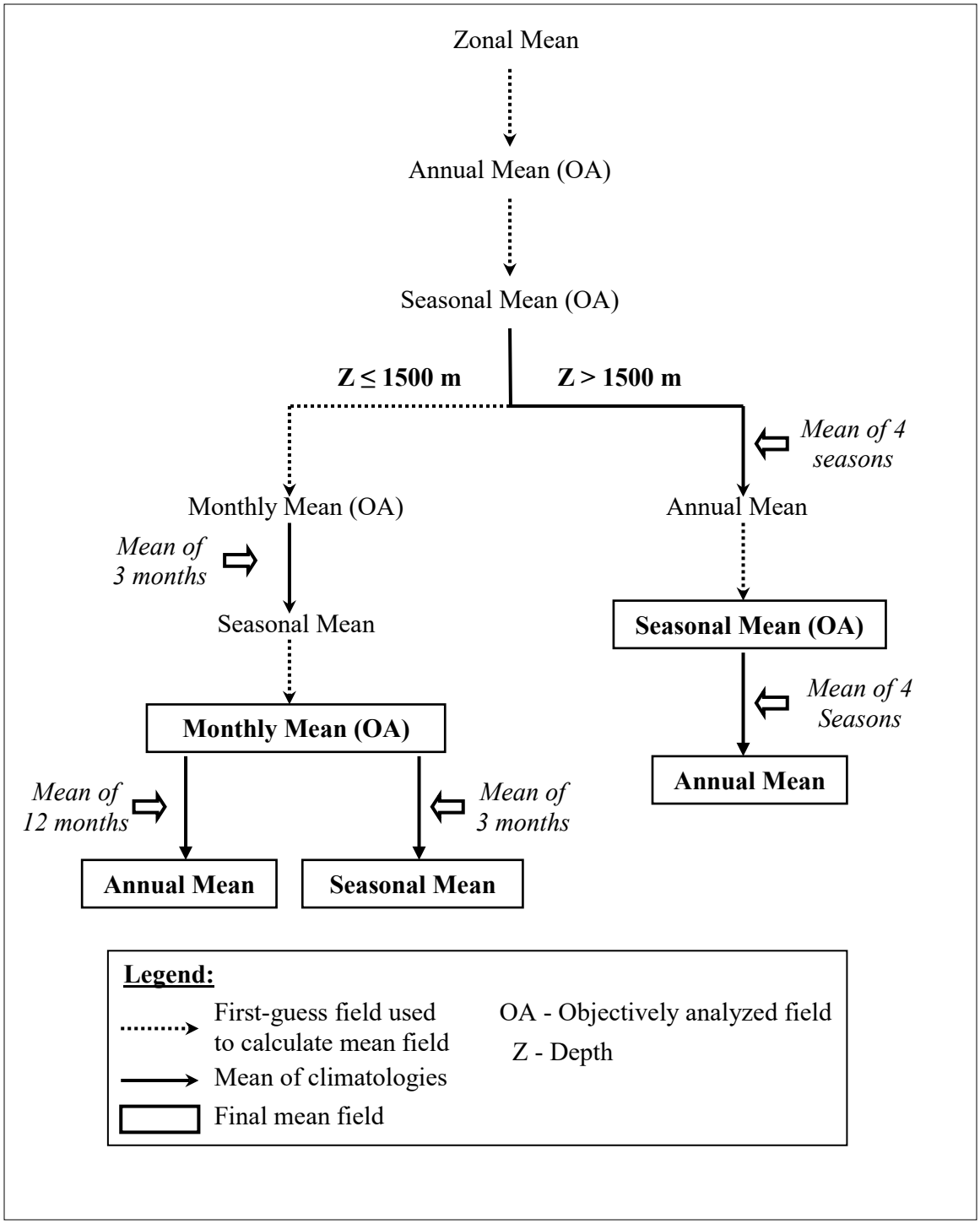

Figure 3. Scheme used in computing "all-data" annual, seasonal, and monthly objectively analyzed means for conductivity.